Sensitivity to Dark Matter Couplings from Frequency Measurements of Acetylene Optical Clocks

Florin Lucian Constantin
Laboratoire PhLAM
CNRS UMR 8523
Villeneuve d'Ascq, France
FL.Constantin@univ-lille1.fr

***Summary*— Couplings of ultralight dark matter candidates to the particles of the Standard Model leading to time variations of the fundamental constants are addressed through measurements of acetylene optical clock transitions. The sensitivity to couplings of ultralight dark matter candidates in the mass range 4.6×10^{-15}–4.6×10^{-6} eV to electrons and photons is evaluated by comparing sub-Doppler and linear absorption $^{12}C_2H_2$ lines of the $\nu_1+\nu_3$ band to a Fabry-Perot cavity-stabilized laser.**

Keywords—acetylene frequency references; sensitivity to proton-electron mass ratio variation; clock comparisons; ultralight dark matter scalar fields; oscillation of fundamental constants

I. INTRODUCTION

The nature of dark matter (mass, spin, couplings) is not known. Ultralight dark matter candidates are scalar classical fields oscillating at the Compton frequency defined by their sub-eV mass. Couplings of these fields to the particles of the Standard Model (SM) induce oscillations of the fundamental constants that translate into oscillations of the atomic, molecular and ultra-stable cavity resonances used as frequency references. Time variation of the fundamental constants [1] was constrained using optical atomic clock comparisons [2] and molecular clock measurements [3]. Constraints on dark matter oscillatory couplings to fundamental constants were derived from atomic clock comparisons [4], from comparisons with lasers locked against optical cavities [5], and recently, from atomic [6] and molecular spectroscopy experiments [7]. Optical fiber links are exploited currently to perform remote clock comparisons by joining together photonics, spectroscopy and fundamental physics [8].

Molecular spectra have intrinsic sensitivity to the nuclear masses. This contribution investigates dark-matter induced oscillations to the fundamental constants by spectroscopy of the acetylene reference transitions in the spectral domain at 1.5 µm [9].

II. ULTRALIGHT DARK MATTER SCALAR FIELDS

A linear coupling of a scalar field ϕ to SM particles is described with a Lagrangian density written as [4,10,11]:

$$L_{int} = \frac{\phi}{\sqrt{2}M_{PI}}\left(\frac{d_\alpha}{4\mu_0}F_{\mu\nu}F^{\mu\nu} + \frac{d_{g_s}\beta(g_s)}{2g_s}G_{\mu\nu}G^{\mu\nu} + -c^2\sum_{X=e,u,d,s}\left(d_{m_X} + \gamma_{m_X}d_{g_s}\right)m_X\Psi_X\overline{\Psi}_X\right). \quad (1)$$

in function of the fermion masses $m_{e,u,d,s}$, fermion spinors $\Psi_{e,u,d,s}$, the anomalous dimension $\gamma_{m_{e,u,d,s}}$ describing the running of the mass of the QCD-coupled fermion, the electromagnetic $F_{\mu\nu}$ and the gluon $G_{\mu\nu}$ fields tensors, and the dimensionless coupling constants $d_\alpha, d_{m_{e,u,d,s}}, d_{g_s}$. The strong interaction is accounted with the coupling constant g_s (with $\alpha_s \equiv g_s^2/4\pi$) and the running function $\beta(g_s)/(2g_s) = -\left(11 - 2\,n_f/3\right)\alpha_s/(8\pi)$ with the energy depending on the number n_f of dynamical quarks. The quantity $M_{PI} = \sqrt{\hbar\,c/(8\pi G)}$ is the reduced Planck mass. A dimensionless scalar field relative to the Plank scale may be defined such as $\varphi = \sqrt{4\pi G/(c\hbar)}\,\phi$.

The field has a quadratic scalar self-interaction potential, normalized such as $V(\varphi) = 2\frac{c^2}{\hbar^2}\left(m_\varphi\varphi\right)^2$ in function of m_φ that has dimension of mass. The potential has an oscillating solution expressed as:

$$\varphi(t,\vec{x}) = \varphi_0 \cdot cos\left(\omega_\varphi t + \vec{k}\vec{x} + \theta\right). \quad (2)$$

The field acts as a pressureless fluid with a non-zero time-averaged energy density [4], that is expressed as $\varrho_\varphi = \frac{c^5}{\hbar^3}m_\varphi^2 M_{PI}^2\varphi_0^2$. This quantity is associated to the local energy density of the dark matter. The interaction with the galactic dark matter halo is described within the standard halo model [12] with an energy density $\rho_{DM} = 0.3\ \mathrm{GeV/cm^3}$, a gaussian velocity distribution around a central velocity $v_{obs} = 230$ km/s and a dispersion characterized through the virial velocity $v_{vir} = 150$ km/s [13]. In function of the speed v of the dark-matter field, the Compton pulsation ω_φ is described with the Doppler-shifted dependence $\omega_\varphi \cong \left(m_\varphi\,c^2/\hbar\right)[1 + v^2/(2c^2)]$ and, wavevector with $\left|\vec{k}\right| \cong m_\varphi\,v/\hbar$. The phase θ is aleatory. The oscillations of the scalar field have a coherence time $\tau \cong 2\pi/\omega_\varphi/(v^2/c^2)$.

The coupling constants may be interpreted as rescaling of five fundamental constants in the SM Lagrangian :

$$\alpha(\varphi) = \alpha(1 + d_e\varphi)$$
$$m_i(\varphi) = m_i\left(1 + d_{m_i}\varphi\right) \quad (3)$$

$$\Lambda(\varphi) = \Lambda\left(1 + d_g\varphi\right)$$

where Λ is the QCD scale parameter. Spacetime dependences of the fundamental constants, showing a modulation by the scalar field $\varphi(t,\vec{x})$, violate the equivalence principle [10]. Following notations in ref.[10], dependences on φ arise on linear combination of the quark masses, namely the mean quark mass $\hat{m}(\varphi) = m_u(\varphi)/2 + m_d(\varphi)/2$ with $d_{\hat{m}} = \left(d_{m_d}m_d + d_{m_u}m_u\right)/(m_d + m_u)$ and the difference of the quark masses $\delta m(\varphi) = m_d(\varphi) - m_u(\varphi)$ with $d_{\delta m} = d_{m_d} - d_{m_u}$. Eq. (3) translates into dependences with φ of the Bohr radius a_0 and of the proton-to-electron mass ratio $\mu = m_p/m_e$ [14]:

$$a_0(\varphi) = \frac{\hbar}{\alpha(\varphi)\cdot cm_e(\varphi)} = a_0\left[1 - \left(d_\alpha + d_{m_e}\right)\varphi\right]$$

$$\mu(\varphi) = \mu\left[1 + \left(d_{m_e} - d_g + 0.037d_{\hat{m}}\right)\varphi\right] \qquad (4)$$

III. Sensitivity to ultralight scalar fields from atomic, molecular and optical reference frequencies

The sizes of atoms and molecules depend linearly with the Bohr radius in the nonrelativistic approximation. A Fabry-Perot cavity based on mirrors separated in vacuum by a distance L defined by an ultra-low-expansion glass spacer displays resonances at harmonics of the free-spectral range with the following scaling relation $f_C \propto c/(2L) \propto c/a_0$.

The variation of the resonance frequency may be parametrized in function of the variations of the fundamental constants such as:

$$\frac{\Delta f_C}{f_C} = Q_\alpha^L\frac{\Delta\alpha}{\alpha} + Q_\mu^L\frac{\Delta\mu}{\mu} \qquad (5)$$

in function of the sensitivity coefficients to the variations of the constants $Q_\alpha^L \cong +1$ (relativistic corrections calculated in [15] are neglected here) and $Q_\mu^L \cong 0$ (as calculated in [15,16]). Note that in this contribution SI units are used and the use of atomic units leads to other values of the sensitivity coefficients to variations of α.

Optical atomic transitions are primarily sensitive to variations in α and m_e. The molecules are additionally sensitive to variations of the nucleon (proton and neutron $m_p \simeq m_n$) masses which are determined primarily by the Λ QCD parameter. The energy levels in molecules may be expressed as the sum between the electronic, the vibrational and the rotational energies $E_{tot} = E_{el} + E_{vib} + E_{rot}$. Spin structure is not taken into account here. At the lowest order of approximation, the electronic energy is expressed as $E_{el} = 2C_{el}hcR_\infty$ where $R_\infty = m_e c\alpha^2/(4\pi\hbar)$ is the Rydberg constant and C_{el} a constant of order unity. Supplementary dependences on the fundamental constants arise from the relativistic corrections to C_{el}, proportional at the lowest order to $\left(Z_{eff}\alpha\right)^2$ where $Z_{eff} \cong 1$ for optical transitions in light molecules, and from corrections for finite nuclear mass to the Rydberg constant, inversely proportional with μ. The vibrational energy is $E_{vib} = hcR_\infty\frac{2C_{vib}}{\sqrt{\mu}}$ with C_{vib} a constant of order unity. Corrections at the lowest order for C_{vib} due to the anharmonicity scale as $1/\mu$, and to the relativistic effects scale as $\left(Z_{eff}\alpha\right)^2$, respectively. Finally, the rotational energy is $E_{rot} = hcR_\infty\frac{C_{rot}}{\mu}J(J+1)$ with C_{rot} a constant of order unity and J the quantum number for the rotational angular momentum. Corrections at the lowest order for C_{rot} scaling as $1/\mu$ are due to the centrifugal distortion, and scaling as $\left(Z_{eff}\alpha\right)^2$ are due to the relativistic effects, respectively.

In general, the variations of nuclear, atomic and molecular transition frequencies may be parametrized in function of the variations of the fundamental constants such as:

$$\frac{\Delta f_{N,A,M}}{f_{N,A,M}} = Q_\alpha^{N,A,M}\frac{\Delta\alpha}{\alpha} + Q_\mu^{N,A,M}\frac{\Delta\mu}{\mu} + Q_q^{N,A,M}\frac{\Delta(\hat{m}/\Lambda)}{\hat{m}/\Lambda} \qquad (6)$$

in function of the sensitivity coefficients to the variations of the fine structure constant $Q_\alpha^{N,A,M}$, proton-to-electron mass ratio $Q_\mu^{N,A,M}$ and quark mass $Q_q^{N,A,M}$. The sensitivity coefficients are calculated using nuclear [14,17,18], atomic [19] and molecular (for a review, see [20]) structure models.

IV. Acetylene : theory, experiments, applications

A. Introduction

Acetylene is a linear molecule in its ground electronic state with $D_{\infty,h}$ symmetry. Acetylene has five vibrational modes $\omega_1\left(\Sigma_g^+\right)$, $\omega_2\left(\Sigma_g^+\right)$ and $\omega_3\left(\Sigma_u^-\right)$ are nondegenerate stretching modes, and $\omega_4\left(\Pi_g\right)$, $\omega_5(\Pi_u)$ are degenerate bending modes. The vibrational and rovibrational energy levels are grouped into clusters (polyads) of interacting energy levels, defined with the following quantum numbers $N_r = 5v_1 + 3v_2 + 5v_3 + v_4 + v_5$, $N_s = v_1 + v_2 + v_3$, and $k = l_4 + l_5$. Acetylene spectra is modelled using a global Hamiltonian (see for example [21]) defined with wavefunctions $|v_1, v_2, v_3, v_4^{l_4}, v_5^{l_5}, J, k\rangle$ expressed with the principal quantum numbers of the harmonic oscillators v_i (i = 1,2,3,4,5), the quantum numbers of the projections of the vibrational angular momentum on the molecular-fixed axis z, arising from the double degenerate normal vibrations l_i (i = 4,5) and the rotational angular momentum quantum number J. Each polyad splits in blocks of energy levels having similar ortho-para and parity symmetries. Alternatively, the energy levels of acetylene and the transition dipole moments may be calculated ab-initio [22]. Acetylene line positions, intensities and broadenings are indicated in databases [23,24]. Acetylene spectroscopy is exploited for many applications, including frequency metrology, astrophysics and environmental science.

B. Variation of fundamental constants from acetylene optical clocks measurements

Acetylene lines, located in the C band of fiber optic telecommunications, are interesting to probe the variability of the fundamental constants by exploiting directly the optical frequency references transferred by fiber links.

Lasers stabilized on saturated absorption lines of acetylene probed by frequency-modulation intracavity spectroscopy and by using the Pound-Drever-Hall stabilization method displayed

a fractional frequency stability of $1.6 \times 10^{-12}\,\tau^{-1/2}$ and a long-term frequency reproducibility of 0.4 kHz on the P(16) reference line of $\nu_1+\nu_3$ band of $^{13}C_2H_2$ [25]. The metrological performances were improved by using fiber lasers up to a fractional frequency stability at $3 \times 10^{-13}\,\tau^{-1/2}$ and to frequency drifts lower than 1 Hz/day [26]. The frequencies of $^{12}C_2H_2$ reference lines and their lineshifts and broadenings were measured with frequency comb techniques [27].

The energy levels of $^{12}C_2H_2$ in the fundamental state [00000] and in the excited states [10100], [$110(11)^{2,0\pm}$] are modeled in the Born-Oppenheimer approximation with a state-of-the-art Hamiltonian that takes into account the rotation, the centrifugal distortion, the vibration, the anharmonicity, the Fermi coupling between [10100] and [$110(11)^0$] states, and the l-type vibrational and rotational interactions in the [$110(11)^{2,0\pm}$] state. Using spectroscopic parameters from literature, the sensitivity coefficients $K_\mu = d(lnf)/d(ln\mu)$ for the rovibrational transitions of the combination bands $\nu_1+\nu_3$ and $\nu_1+\nu_2+\nu_4+\nu_5$ are calculated and displayed in Figure 1 [28].

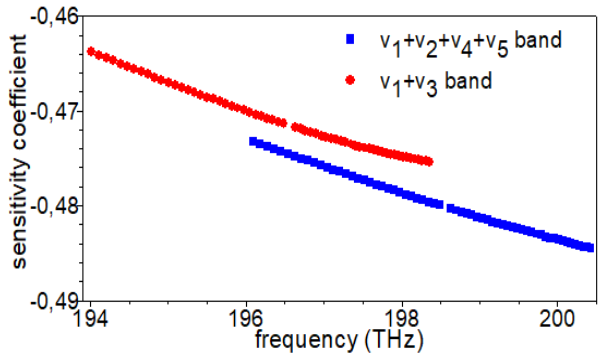

Fig. 1. Sensitivity coefficients for $^{12}C_2H_2$ reference transitions.

The frequency measurements of $^{12}C_2H_2$ transitions against the Cs primary standard are probes for the variations of the fundamental constants:

$$\frac{\Delta(f_{C_2H_2}/f_{Cs})}{f_{C_2H_2}/f_{Cs}} = (K_\mu - 1)\frac{\Delta\mu}{\mu} - 0.83\frac{\Delta\alpha}{\alpha} + 0.046\frac{\Delta(m_e/\Lambda)}{m_e/\Lambda} \quad (1)$$

100 absolute frequency measurements of the P(16) of $\nu_1+\nu_3$ band clock transition performed at equal time intervals during one year are simulated assuming 100 Hz C_2H_2 optical clock frequency uncertainty. The slope of the fractional time variation of the absolute frequency is 2×10^{-13}/yr. Assuming only μ variation, that translates into a constraint at 4×10^{-13}/yr.

C. *Atmospheric science*

Spectroscopy of acetylene enables many applications, for example, in atmospheric science [29], astrophysics [30], combustion science [31], and temperature metrology [32].

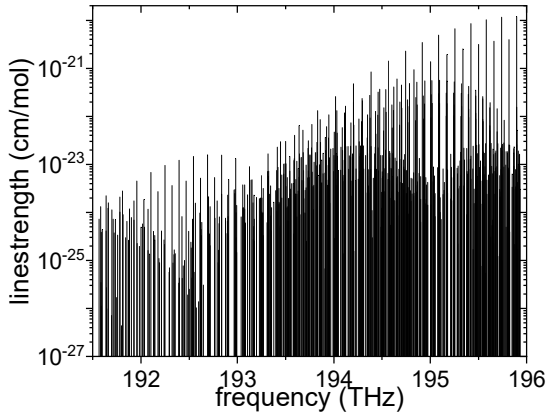

Fig. 2. Linestrengths of $^{12}C_2H_2$ transitions in the C band.

Direct absorption spectroscopy in the gas phase presents many advantages for sensing applications: calibration-free measurements of species concentrations, their time dependence characterization and the temperature measurement. Acetylene displays a dense spectrum of intense lines in the C band used in optical telecommunications [24] which are indicated in Figure 2. Tunable diode laser spectroscopy in a multi-pass cell using a modulation technique enabled highly sensitive detection of acetylene transitions at 1.5 µm [33]. Multispecies monitoring was achieved with a sensitivity at concentrations below the ppm level for 1 s integration time and at tens of ppb after averaging up to the 100 s timescale [34]. Figure 3 displays the spectra calculated for different species relevant for atmospheric science [24] in a spectral range of 60 GHz centered on the frequency of the REFIMEVE optical fiber link reference signal. The spectra are calculated with the reference data from the HITRAN database by using the Voigt profile for a temperature of 300 K and a pressure of 6,7 kPa.

V. Experimental Principle and Sensitivity

Oscillations of fundamental constants are probed by monitoring the fractional variation between the frequency of a Fabry-Perot stabilized laser f_L and the frequency of an acetylene transition f_{mol}:

$$\frac{f_L - f_{mol}}{f_L} = (Q_\alpha^L - Q_\alpha^{mol})\frac{\Delta\alpha}{\alpha} + (Q_\mu^L - Q_\mu^{mol})\frac{\Delta\mu}{\mu} \quad (7)$$

The laser and the molecular frequency display different sensitivities to the variations of the fundamental constants, quantified through the relevant sensitivity coefficients $Q_{\alpha,\mu}^{L,mol}$.

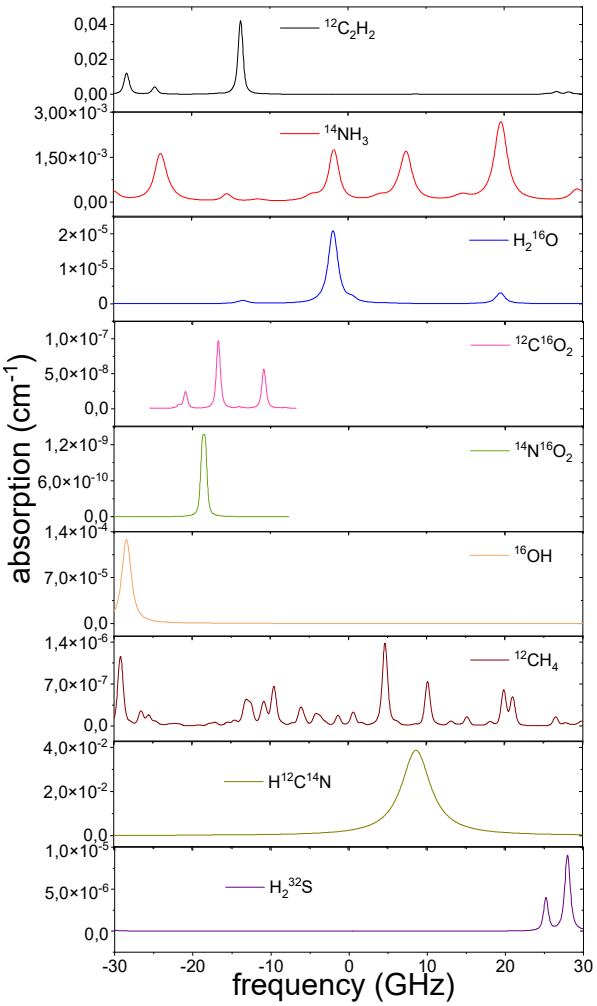

Fig. 3. Calculated spectra of selected molecular transitions in function of the frequency shift to the REFIMEVE optical reference.

The response time of the experimental setup to perturbations limits the sensitivity to the oscillations of the fundamental constants [35]. On one hand, the frequency of the laser locked to the Fabry-Perot cavity follow perturbations up to a frequency imposed by acoustic wave propagation in the ultra-low-expansion glass spacer of the cavity, that is $f_{c1} =$ 27 kHz for the REFIMEVE reference cavity [36]. The response function is $h_L\left(f_\varphi\right) = 1\ if\ f_\varphi < f_{c1}, 0\ if\ f_\varphi \geq f_{c1}$. On the other hand, the molecular response decreases for oscillations at timescales shorter than the molecular coherence time. For radiative or collisional broadened lines, that is the inverse of the linewidth (full width half measured) in non-angular frequency units. Two experimental setups are investigated here. The experimental setup A addresses Doppler-free saturated absorption lines of $^{12}C_2H_2$ investigated at conditions recommended by the CCL/BPIM to setup a standard. The collisional broadening is dominant and a cutoff frequency $f_{c2,A} = 600$ kHz is estimated using results from [37]. The experimental setup B addresses linear absorption in a high-pressure $^{12}C_2H_2$ gas cell (66.7 kPa). The collisional broadening is dominant and a cutoff frequency $f_{c2,B} = 4$ GHz is estimated using results from [38]. The response function, assumed here as $h_{mol}\left(f_\varphi\right) = 1/\sqrt{1+\left(\frac{f_\varphi}{f_{c2}}\right)^2}$, may be calibrated experimentally. Inserting the response functions in Eq. (7), one obtains:

$$\frac{f_L(t)-f_{mol}(t)}{f_{L(t)}} = \left(Q_\alpha^L h_L\left(f_\varphi\right) - Q_\alpha^{mol} h_{mol}\left(f_\varphi\right)\right)\frac{\Delta\alpha(t)}{\alpha} + \left(Q_\mu^L h_L\left(f_\varphi\right) - Q_\mu^{mol} h_{mol}\left(f_\varphi\right)\right)\frac{\Delta\mu(t)}{\mu} \quad (8)$$

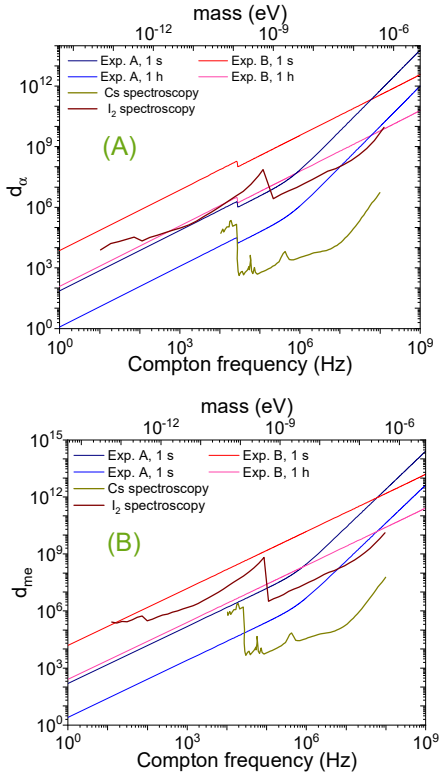

Fig. 4. Constraints for dark-matter couplings to α (A) and m_e (B).

The stabilized laser signal used in this experiment is the REFIMEVE optical reference, based on a continuous-wave erbium-doped fiber-laser emitting at 1542.14 nm stabilized on a Fabry–Perot cavity and referenced to a hydrogen maser at SYRTE (Observatoire de Paris) [39]. The fractional stability is better than 10^{-15} up to 10^5 s of averaging time. The laser is transferred through single mode fiber of the optical telecommunications network to PhLAM (Université de Lille) with length of 2×340 km. The noise arising from propagation in the fiber is actively compensated [40,41] that enables delivering almost continuously an optical signal at 194,400,084,500.000(25) kHz. The experiment aim to investigate the P(27) transition of the ν_1+ν_3 band of $^{12}C_2H_2$, measured at 194,386,332,283.6(2.0) kHz in Madej *et al* [27], that is the nearest acetylene reference transition to the optical reference signal. Frequency-shifting the REFIMEVE signal by

-13.752 GHz to interrogate this transition may be conveniently performed with lithium niobate waveguide optical modulators.

The sensitivity coefficients in Eq. (7) are $Q_\alpha^L \cong 1, Q_\mu^L \cong 0$ and $Q_\alpha^{mol} \cong 2, Q_\mu^{mol} \cong -0.47$. The frequency deviation will be translated in the experiment with the photodetector to a voltage signal that will be recorded by fast data acquisition system and averaged. The noises limiting the sensitivity of detection of dark-matter-induced oscillations come from the reference optical signal, the molecular line, and from the detection chain. Here it is assumed that the frequency measurements may be performed with fractional uncertainties with dependences assumed as $(\Delta f/f)_A(\tau) = 10^{-14}(\tau/1\ \mathrm{s})^{-1/2}$, for sub-Doppler spectroscopy, and $(\Delta f/f)_B(\tau) = 10^{-12}(\tau/1\ \mathrm{s})^{-1/2}$, in linear spectroscopy, in function of the averaging time τ in seconds. These uncertainties combined with the experimental response functions are exploited to set up upper bounds on the couplings of scalar fields to the fine structure constant or to the electron mass, using Eqs. (3,4,8) and by neglecting couplings to other fundamental constants. The bounds calculated for the Galactic halo of dark matter are shown in Figure 4. Addressing both A and B experiments enables probing a Compton frequency range improved by an order a magnitude comparing to the previous Cs [6] and I_2 [7] spectroscopy experiments. Averaging may lead to record results, notably for frequencies less than 10 kHz level. The finite coherence time of the Galactic halo will limit the averaging time when detecting fast oscillations of the fundamental constants.

VI. Conclusions

Spectroscopy of the reference transitions of acetylene may be exploited to constrain coupling of ultralight dark matter scalar fields to the SM particles. Comparing to the previous experiments in atomic and molecular spectroscopy, this approach combining sub-Doppler and linear absorption spectroscopy measurements may improve the frequency bounds probed for the scalar field-induced oscillations by an order of magnitude. In addition, this approach may improve the constraints to the couplings of the scalar fields to the fine structure constant and to the electron mass for Compton frequencies from Hz to tens of kHz.

Acknowledgement

This work is supported by the *Programme National GRAM* of CNRS/INSU and partly by the French ANR agency under contract No. ANR-11-LabX-0005-01 CaPPA (Chemical and Physical Properties of the Atmosphere). Laboratoire PhLAM is member of the Equipex+ T-REFIMEVE (French contract *PIA 3 Equipements Structurants pour la Recherche* of the Ministry of Higher Education, Research and Innovation and the General Secretariat for the Investment Plan).

References

[1] J.-Ph. Uzan, "Varying constants, gravitation and cosmology," Living Rev. Relativ., vol. 14, pp. 2, March 2011.

[2] R.M. Godun *et al*, "Frequency ratio of two optical clock transitions in $^{171}Yb^+$ and constraints on the time variation of fundamental constants," Phys. Rev. Lett., vol. 113, pp. 210801, November 2014; W.F. McGrew *et al*, "Towards the optical second: verifying optical clocks at the SI limit," Optica, vol. 6, pp. 448–454, April 2019; R. Lange *et al*, "Improved limits for violations of local position invariance from atomic clock comparisons," Phys. Rev. Lett., vol. 126, pp. 011102, January 2021.

[3] A. Shelkovnikov, R.J. Butcher, C. Chardonnet, and A. Amy-Klein, "Stability of the proton-to-electron mass ratio," Phys. Rev. Lett., vol. 100, pp. 150801, April 2008; J. Kobayashi, A. Ogino, and S. Inouye, "Measurement of the variation of electron-to-proton mass ratio using ultracold molecules produced from laser-cooled atoms," Nat. Commun., vol. 10, pp. 3771, August 2019.

[4] A. Hees *et al*, "Searching for an oscillating massive scalar field as a dark matter candidate using atomic hyperfine frequency comparisons," Phys. Rev. Lett., vol. 117, pp. 061301, August 2016.

[5] P. Wcisło *et al*, "New bounds on dark matter coupling from a global network of optical atomic clocks," Sci. Adv., vol. 4, pp. eaau4869, December 2018; C.J. Kennedy *et al*, "Precision metrology meets cosmology: improved constraints on ultralight dark matter from atom-cavity frequency comparisons," Phys. Rev. Lett., vol. 125, pp. 201302, November 2020.

[6] O. Tretiak *et al*, "Improved bounds on ultralight scalar dark matter in the radio-frequency range," Phys. Rev. Lett., vol. 129, pp. 031301, July 2022.

[7] R. Oswald *et al*, "Search for dark-matter-induced oscillations of fundamental constants using molecular spectroscopy," Phys. Rev. Lett., vol. 129, pp. 031302, July 2022.

[8] C. Clivatti *et al*, "Coherent optical-fiber link across Italy and France," Phys. Rev. Appl., vol. 18, pp. 054000, November 2022.

[9] Recommandation CCL 1, 2009 Comité Consultatif des Longueurs, 13th Meeting 32–6 (2007), www.bipm.org/en/committees/cc/ccl/publications-cc.html.

[10] T. Damour and J.F. Donoghue, "Equivalence principle violations and couplings of a light dilaton," Phys. Rev. D, vol. 82, pp. 084033, October 2010.

[11] A. Arvanitaki, J. Huang, and K. Van Tilburg, "Searching for dilaton dark matter with atomic clocks," Phys. Rev. D, vol. 91, pp. 015015, January 2015.

[12] P.J. MacMillan, "Mass models of the Milky Way," Monthly Notices of the Royal Astronomical Society, vol. 414, pp. 2446–2457, June 2011.

[13] J.W. Foster, N.L. Rodd, and B.R. Safdi, "Revealing the dark matter halo with axion direct detection," Phys. Rev. D, vol. 97, pp. 123006, June 2018.

[14] V.V. Flambaum, D.B. Leinweber, A.W. Thomas, and R.D. Young, "Limits on variations of the quark masses, QCD scale, and fine structure constant," Phys. Rev. D, vol. 69, pp. 115006, June 2004.

[15] L.F. Pašteka *et al*, "Material size dependence on fundamental constants," Phys. Rev. Lett., vol. 122, pp. 160801, April 2019.

[16] Y.V. Stadnik and V.V. Flambaum, "Enhanced effects of variation of the fundamental constants in laser interferometers and application to dark-matter detection," Phys. Rev. A, vol. 93, pp. 063630, June 2016.

[17] V.V. Flambaum and A.F. Tedesco, "Dependence of nuclear magnetic moments on quark masses and limits on temporal variation of fundamental constants from atomic clock experiments," Phys. Rev. C, vol. 73, pp. 055501, May 2006.

[18] P. Fadeev, J.C. Berengut, and V.V. Flambaum, "Effects of variation of the fine structure constant α and quark mass m_q in Mössbauer nuclear transitions," Phys. Rev. C, vol. 105, pp. 051303, May 2022.

[19] V.A. Dzuba and V.V. Flambaum, "Relativistic corrections to transition frequencies of AgI, DyI, HoI, YbII, YbIII, AuI, and HgII and search for variation of the fine-structure constant," Phys. Rev. A, vol. 77, pp. 012515, January 2008; J.C. Berengut, V.A. Dzuba, and V.V. Flambaum, "Transitions in Zr, Hf, Ta, W, Re, Hg, Ac, and U ions with high sensitivity to variation of the fine-structure constant," Phys. Rev. A, vol. 84, pp. 054501, November 2011; M.S. Safronova *et al*, "Highly charged ions for atomic clocks, quantum information, and search for α variation," Phys. Rev. Lett., vol. 113, pp. 030801, July 2014.

[20] P. Jansen, H.L. Bethlem, and W. Ubachs, "Perspective: Tipping the scales: Search for drifting constants from molecular spectra," J. Chem. Phys., vol. 140, pp. 010901, January 2014.

[21] M. Herman and D.S. Perry, "Molecular spectroscopy and dynamics: a polyad-based perspective," Phys. Chem. Chem. Phys., vol. 15, pp. 9949–10516, July 2013; O.M. Lyulin and V.I. Perevalov, "Global modeling of

vibration-rotation spectra of the acetylene molecule," J. Quant. Spectrosc. Radiat. Transf., vol. 177, pp. 59–74, July 2016.

[22] K.L. Chubb *et al*, "MARVEL analysis of the measured high-resolution rovibrational spectra of C_2H_2," J. Quant. Spectrosc. Radiat. Transf., vol. 204, pp. 42–55, January 2018.

[23] N. Jacquinet-Husson *et al*, "The 2015 edition of the GEISA spectroscopic database," J. Mol. Spectrosc., vol. 327, pp. 31–72, September 2016.

[24] I.E. Gordon *et al*, "The HITRAN2020 molecular spectroscopic database," J. Quant. Spectrosc. Radiat. Transf., vol. 277, pp. 107949, January 2022.

[25] C.S. Edwards *et al*, "High-accuracy frequency atlas of $^{13}C_2H_2$ in the 1.5 μm region," Appl. Phys. B, vol. 80, pp. 977–983, June 2005.

[26] T. Talvard *et al*, "Enhancement of the performance of a fiber-based frequency comb by referencing to an acetylene-stabilized fiber laser," Opt. Express, vol. 25, pp. 2259–2269, Feb. 2017.

[27] C.S. Edwards *et al*, "High precision frequency measurements of the $\nu_1 + \nu_3$ combination band of $^{12}C_2H_2$ in the 1.5 μm region," J. Mol. Spectrosc., vol. 234, pp. 143–148, November 2005; A.A. Madej *et al*, "Accurate absolute reference frequencies from 1511 to 1545 nm of the $\nu_1 + \nu_3$ band of $^{12}C_2H_2$ determined with laser frequency comb interval measurements," J. Opt. Soc. Am. B, vol. 23, pp. 2200–2208, October 2006; S. Twagirayezu, G.E. Hall, and T.J. Sears, "Frequency measurements and self-broadening of subDoppler transitions in the $\nu_1 + \nu_3$ band of C_2H_2," J. Chem. Phys., vol. 149, pp. 154308, October 2018.

[28] F.L. Constantin, "Sensitivity to electron-to-proton mass ratio variation from $^{12}C_2H_2$ rovibrational transitions to $\nu_1+\nu_3$ and $\nu_1+\nu_2+\nu_4+\nu_5$ interacting levels," Vibrational Spectroscopy, vol. 85, pp. 228–234, July 2016.

[29] R.A Whitby and E.R Altwicker, "Acetylene in the atmosphere: Sources, representative ambient concentrations and ratios to other hydrocarbons," Atmospheric Environment, vol. 12, pp. 1289–1296, December 1967.

[30] K. Didriche and M. Herman, "A four-atom molecule at the forefront of spectroscopy, intramolecular dynamics and astrochemistry: Acetylene," Chem. Phys. Lett., vol. 496, pp. 1–7, August 2010.

[31] A. Castrillo *et al*, "Optical determination of thermodynamic temperatures from a C_2H_2 line-doublet in the near infrared," Phys. Rev. Appl., vol. 11, pp. 064060, June 2019.

[32] S. Wagner *et al*, "In situ TDLAS measurement of absolute acetylene concentration profiles in a non-premixed laminar counter-flow flame," Appl. Phys. B, vol. 107, pp. 585–589, March 2012.

[33] Haiyue Sun *et al*, "Highly sensitive acetylene detection based on a compact multi-pass gas cell and optimized wavelength modulation technique," Infrared Physics & Technology, vol. 102, pp. 103012, November 2019.

[34] W. Duan *et al*, "A laser-based multipass absorption sensor for sub-ppm detection of methane, acetylene and ammonia," Sensors, vol. 22, pp. 556, December 2022.

[35] K. Van Tilburg, N. Leefer, L. Bougas, and D. Budker, "Search for ultralight scalar dark matter with atomic spectroscopy," Phys. Rev. Lett., vol. 115, pp. 011802, June 2015.

[36] E. Savalle *et al*, "Searching for dark matter with an optical cavity and an unequal-delay interferometer," Phys. Rev. Lett., vol. 126, pp. 051301, February 2021.

[37] J. Hald *et al*, "Fiber laser optical frequency standard at 1.54 μm," Opt. Express, vol. 19, pp. 2052–2063, January 2011.

[38] W.C. Swann and S.L. Gilbert, "Pressure-induced shift and broadening of 1510–1540-nm acetylene wavelength calibration lines," J. Opt. Soc. Am. B, vol. 17, pp. 1263–1270, July 2000.

[39] X. Xie *et al*, "Phase noise characterization of sub-hertz linewidth lasers via digital cross correlation," Opt. Lett., vol. 42, pp. 1217–1220, April 2017.

[40] D. Xu *et al*, "Studying the fundamental limit of optical fiber links to the 10^{-21} level," Opt. Express, vol. 26, pp. 9515–9527, April 2018.

[41] E. Cantin *et al*, "An accurate and robust metrological network for coherent optical frequency dissemination," New J. Phys., vol. 23, pp. 053027, May 2021.